COMPACT COPPER/EPOXY-BASED ELECTROMAGNETIC SCANNER FOR SCANNING PROBE APPLICATIONS

H. Rothuizen, M. Despont, U. Drechsler, G. Genolet, W. Häberle, M. Lutwyche, R. Stutz, and P. Vettiger
IBM Research, Zurich Research Laboratory, 8803 Rüschlikon, Switzerland

ABSTRACT

We report on the fabrication of a flat *X/Y/Z* microscanner that uses flexible rubber posts as a spring system and planar coils embedded in an epoxy body for electromagnetic actuation. The device is primarily intended for motion in the *X-Y* plane, in which it can scan a 100 µm displacement range with about 3 mW of power. Various shapes of the posts are considered in order to adjust the ratios of stiffnesses for in-plane and out-of-plane motion.

INTRODUCTION

New directions in scanning probe techniques are low-cost, portable imaging systems [1,2] and parallel operation of multiple probes for fast imaging, lithography, and storage applications [3,4]. A key issue is the need for a low-cost, miniaturized scanner with *X/Y/Z* motion capabilities and a lateral scanning range on the order of 100 µm. Multiple probe systems arranged as 1D or 2D arrays [4] must also be able to control, by tilt capabilities, the parallelism between the probe array and the sample.

We have developed a microscanner with these properties based on electromagnetic actuation. It consists of a mobile platform, supported by springs and containing integrated planar coils, which is positioned over a set of miniature permanent magnets [5]. A suitable arrangement of the coils and magnets allows us, by electrically addressing the different coils, to apply magnetically induced forces to the platform and drive it in the *X,Y,Z* and tilt directions. Our first silicon/copper-based version of this device has proved the validity of the concept [6], and variations of it have since been used elsewhere [7]. However, the fabrication was found to be costly due to a deep trench etching step, and made difficult by the brittleness of silicon. Furthermore, the undamped copper spring system gave rise to excessive cross talk and ringing when driven in an open loop, and its layout limited the compactness of the overall device.

In this paper we investigate a modified microscanner that uses flexible rubber posts as a spring system and a copper/-epoxy-based mobile platform, Fig. 1. The platform is made of a thick, epoxy-based SU-8 resist [8] in which the copper coils are embedded. The posts are made of polydimethylsiloxane (PDMS) and are fastened at the corners of the platform and at the ground plate, providing an optimally compact device by sharing the space below the platform with the magnets. The shape of the posts allows their lateral and longitudinal stiffness to be adjusted, and the dissipative rubber-like properties of PDMS provide damping to avoid platform ringing and to suppress nonlinearities.

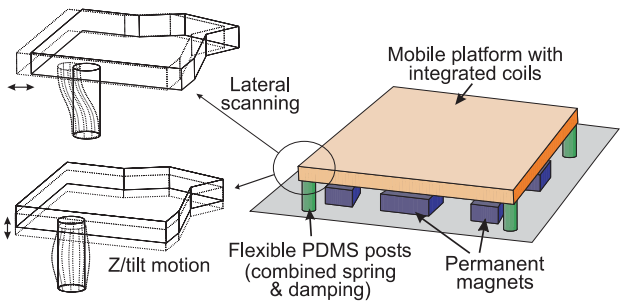

Figure 1. Microscanner concept, using a mobile platform and flexible posts.

DESIGN

Our primary concern, as a differentiator to conventional scanning probe actuators, is to obtain a large ratio of in-plane range to device volume. Figure 2 shows the layout of the platform, which is scaled laterally so that the long segments of the "racetrack" coils used for in-plane actuation coincide with commercially available 2×4 mm^2 SmCo magnets. The thickness of the device is determined by that of the magnets (1 mm), the clearance between magnet and platform (500 µm), and the thickness of the platform itself, which is 250 µm and determined mainly by the aspect ratio achievable in SU-8 resist during the exposure of the coil plating mold. The resulting device volume is approximately 15×15×1.6 mm^3.

For a coil layout similar to that in Fig. 2, the amplitude of the Lorentz force which drives in-plane actuation is $F_{X,Y} = BIL_{\text{eff}}$, where B is the average magnetic field intensity throughout the thickness of the coil, I the coil current, and L_{eff} the effective length of coil wire contributing to the actuation. Our SmCo magnets produce a measured magnetic field intensity of ≃ 0.14 T at the mid-thickness of the coils. The effective coil length is 320 mm, yielding an expected force $F_{X,Y}$ of 45 µN per milliamp of drive current.

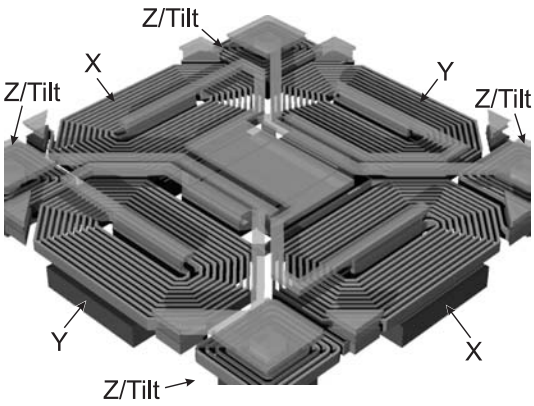

Figure 2. Arrangement of the coils, the interconnects and the permanent magnets, as well as the various motions addressed by the corresponding coils.

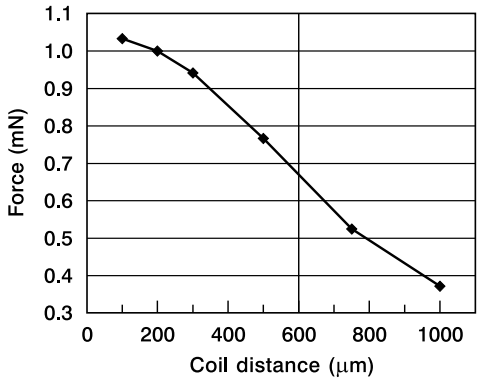

Figure 3. Force versus distance relationship for the magnet-and-coil geometry used for *Z*-actuation at a coil drive current of 100 mA. The magnet is 2×2×1 mm^3 and magnetized along its short length with a strength adjusted to fit the magnetic field intensity of 0.1 T measured at a distance of 500 μm. The planar coil is positioned coaxially with the field generated by the magnet. It is square, with an inner dimension of 1.1 mm, an outer dimension of 3.3 mm, 18 turns, and a thickness of 200 μm. The coil distance refers to the offset from the surface of the magnet to the mid-thickness of the coil. These calculations were made using a 3D scalar potential method in ANSYS™.

To estimate the out-of-plane force, we resort to a finite element analysis of the magnetostatics of the coaxial coil-and-magnet system used for *Z*-actuation at the corners of the platform. Figure 3 shows a calculated force-distance curve from which, the force being proportional to the coil current, we expect an out-of-plane force F_Z of 6.7 μN per milliampere of drive current at the working magnet-to-coil distance of 600 μm.

The principal design issue of the spring system is the ratio of its stiffnesses for in-plane and out-of-plane motion. Whereas for many scanning probe applications the required *Z*-axis range does not need to be much larger than a few microns, it is necessary to ensure that the *Z*-axis retraction of the platform due to the shortening of the posts as they take on an "S" shape at large in-plane deflections can be compensated for at acceptable *Z*-coil current levels. Figure 4 shows a set of various PDMS post shapes, and Table 1 lists their relative stiffnesses and *Z*-retraction at 50 μm in-plane deflection. Spring types 3 and 4 illustrate the ability to design shapes that increase the out-of-plane range without significantly affecting the in-plane behavior, compared to a simple straight post (type 2), see also Fig. 5. Our original cylindrical version of the post (type 1) is clearly too stiff as it would require more than 1 A of drive current to obtain a DC deflection of 50 μm.

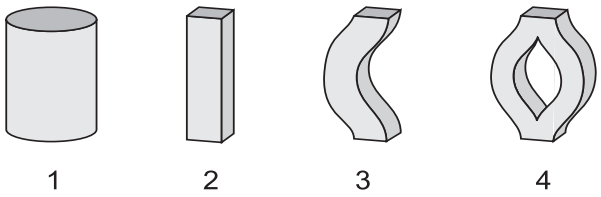

Figure 4. Shapes of molded PDMS used for the spring system. All posts are 1.2 mm high and 300×300 μm^2 in cross-section at their base and top, except for type 1, which is a cylinder of diameter 850 μm.

Table 1. Calculated stiffnesses $k_{X,Y}$ and k_Z for the shapes in Fig. 4 using a Young's modulus of 3.5 MPa and a Poisson's ratio of 0.33 for the PDMS material [9]. The quantity ΔZ is the (average) *Z*-retraction of the platform for an in-plane deflection of 50 μm obtained by applying an in-plane force of magnitude $F_{X,Y,50}$, and $F_{Z,50}$ is the out-of-plane force required to compensate for the same platform *Z*-retraction. These values are for the full four-post spring system, and non-axissymmetric shapes are oriented such that their extruded length is along the *Y*-axis. The calculations were made using the ANSYS™ finite element analysis tool, taking into account large deformation nonlinearities.

Post shape	$k_{X,Y}$ (N/m)	k_Z (N/m)	ΔZ (μm)	$F_{X,Y,50}$ (mN)	$F_{Z,50}$ (mN)
1	1,200	4,400	–1.06	60	4.7
2	60	886	–3.75	3	3.3
3	50(*X*), 45(*Y*)	422	–6.88	2.5(*X*), 2.3(*Y*)	2.9
4	40(*X*), 60(*Y*)	419	–7.04	2.0(*X*), 3.0(*Y*)	2.9

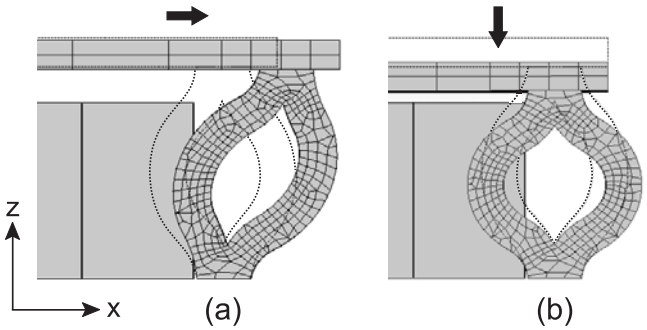

Figure 5. Deformations of type-4 post for (a) an in-plane and (b) an out-of-plane force of 3 mN and applied to the platform [the deformations are amplified by a factor of 5 for (a) and 20 for (b)]. The dotted lines show the positions of platform and post at rest.

FABRICATION

The fabrication sequence, Fig. 6, starts on a silicon wafer with a seed layer and a lithographically patterned 200-μm-thick SU-8 layer in which copper is electroplated to form the coils (Fig. 6a). The coils typically have 20 turns, with a pitch of 100 μm and a spacing of 20 μm. Special care was taken in the resist processing and platform design to achieve the necessary aspect ratio and to overcome adhesion and stress problems of SU-8. A second SU-8 layer, which serves as an insulator, is patterned with via holes, and another seed layer is then deposited (Fig. 6b). Next, an interconnect level is formed using a Novolac-type resist mask and a second copper electroplating step (Fig. 6c). After stripping the re-

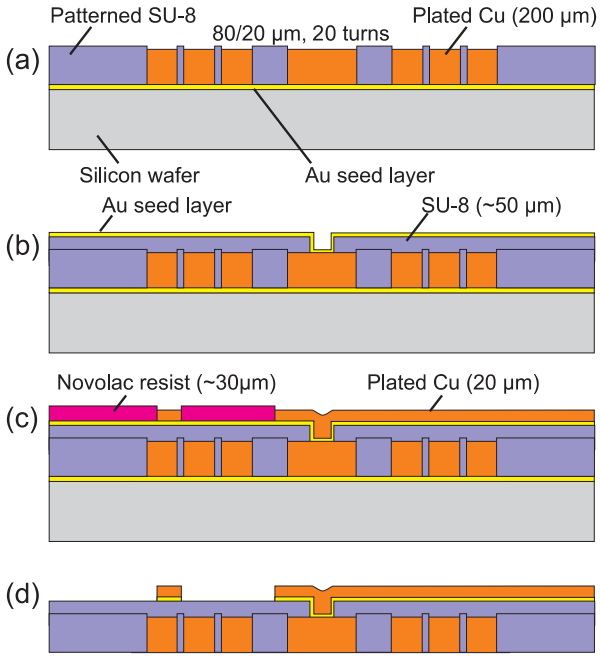

Figure 6. Cross section of the platform fabrication process. (a) Coils are electroplated through an SU-8 resist mask, which is kept as the body of the platform; (b) an insulator layer is deposited; (c) interconnects are electroplated; (d) the platform is released from the silicon substrate.

sist, the silicon wafer is dissolved by a sequence of wet and dry etching, and the exposed seed layers are sputtered away to prevent shorts (Fig. 6d).

Rubber posts for the spring system are fashioned by curing the liquid PDMS precursor in an appropriate mold. For cylindrical posts, the liquid is hardened in a glass capillary. For more complex, "extruded" shapes such as those discussed below, the liquid is hardened in a DRIE-etched silicon master, and then demolded. After that, the individual posts are separated from the bulk PDMS by cutting them out flush with the silicon master imprint surface.

Finally, 20 µm diameter gold leads are bonded to the platform contacts, and all the components (platform, posts, and magnets) are assembled by gluing with a fast-curing epoxy to a planar base plate. The latter operation incurs some shortening of the PDMS posts due to a meniscus of glue at their base, but this is precompensated for by slightly lengthening the shapes in the silicon master. Figure 7 is an optical top view of a finished microscanner.

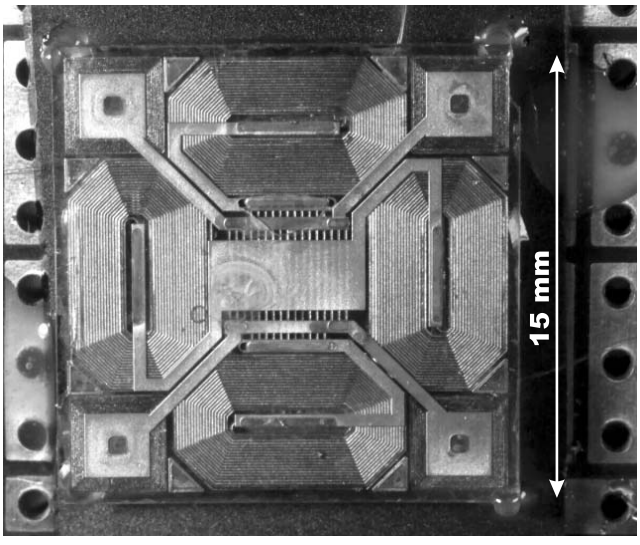

Figure 7. Optical top view of a fabricated microscanner.

RESULTS

The motion of the scanner was characterized using a microvision strobe technique [10]. Frequency response curves for in-plane motion (Fig. 8) show broad peaks (characteristic of a large degree of damping) at frequency values that are consistent with expectations based on the usual formula $f = (1/2\pi)\sqrt{k/m}$, using the values listed in Table 1 and the measured mass of the platform (0.253 mg). The spring type 2 response presents a shoulder at about 100 Hz, which reflects that there is some mixing on resonance between the *X* and *Y*-axes through a yaw-type motion (rotation about the *Z*-axis). This behavior is linked to an imperfect decoupling of the *X* and *Y*-axes that is inherent in the spring geometry, but it does not occur off resonance and therefore has no detrimental effect for operation at typical scanning probe frequencies of up to 10 Hz. The amplitude response (Fig. 9) displays the excellent linearity of the spring system for displacement amplitudes up to 80 µm (160 µm displacement range). Based on these near-DC (10 Hz) responses and a measured circuit resistance of 1.9 Ω, the power necessary for a 50 µm displacement is 2.7 mW in the case of the softer spring system.

Owing to limitations of the measurement technique, it was not possible to measure driven out-of plane displacements greater than 0.5 µm. However, the small-amplitude response for *Z*-motion when all four corner coils are driven in-phase also displays good linearity over the range that can be measured (Fig 10). Although the actual displacement obtained is smaller than the value expected from our esti-

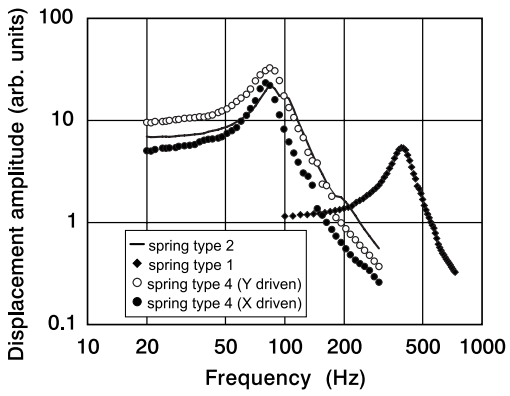

Figure 8. Frequency response for in-plane motion (*X* and *Y* axis are equivalent for spring types 1 and 2). The mechanical quality factors measured are between 3.3 and 4.6.

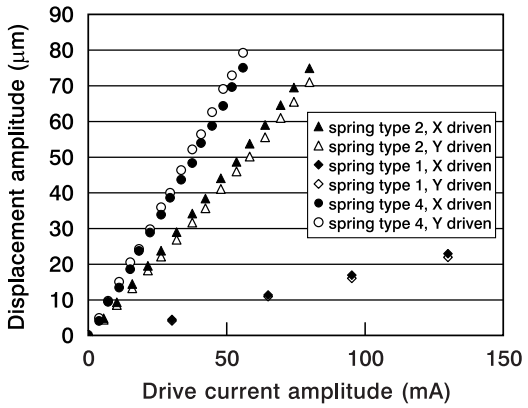

Figure 9. In-plane displacement amplitude response for an AC drive current at 10 Hz (off resonance) for spring types 2 and 4, and at 400 Hz (near resonance) for spring type 1.

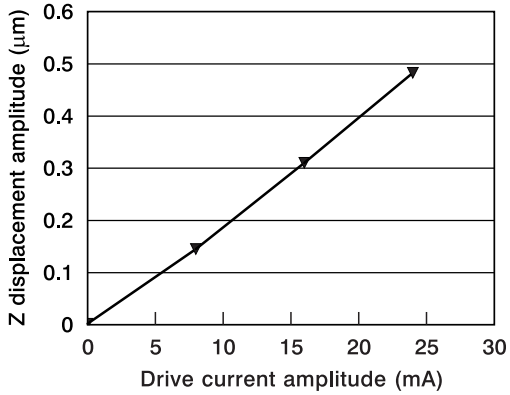

Figure 10. Out-of-plane amplitude response for an AC drive current at 3 Hz and a type-4 spring system. The drive current is the total for all four corner coils, which are driven in phase.

mates of the force and stiffness (0.480 μm instead of 0.77 μm at 48 mA drive current), the discrepancy is still well within acceptable limits when one considers that the electrical leads to the platform have been neglected so far, and that although they are negligible in mass, they may well contribute to stiffen the spring system.

CONCLUSION

The electromagnetic scanner we have fabricated performs predictably and well in terms of the scan range, device volume, and power requirements, achieving displacement ranges of 100 μm with approximately 3 mW of power. By being potentially cheap to manufacture, it presents a good alternative actuation system for many scanning probe applications. It does, however, have one disadvantage: the price for its compactness is a relatively large *Z*-retraction of the platform, which generally has to be compensated for by active use of the *Z*-actuation, rather than passively as it is currently done in conventional scanners based on piezoresistive tubes. For applications involving arrayed probes, this overhead is no longer detrimental because an active use of tilt degrees of freedom is often necessary for leveling purposes anyway.

ACKNOWLEDGMENT

The authors thank M. Lantz**,** G. Binnig, U. Dürig, B. Gotsmann, R. Widmer, and P. F. Seidler for their support and helpful discussions during the course of this work.

REFERENCES

[1] SII Nanopics® Brochure, 1998.
[2] Nanosurf® Brochure, 1999.
[3] S.C. Minne, G. Yaralioglu, S. R. Manalis, J. D. Adams, A. Atalar, and C.F. Quate, "Automated Parallel High-Speed Atomic Force Microscopy", Appl. Phys. Lett. 72, 2340-2342 (1998).
[4] P. Vettiger, M. Despont, U. Drechsler, U. Dürig, W. Häberle, M. I. Lutwyche, H. Rothuizen, R. Stutz, R. Widmer and G. K. Binnig, "The "Millipede"- More than one Thousand Tips for Future AFM Data Storage", IBM J. Res. Develop. 44, 323-340 (2000).
[5] M. Lutwyche, U. Drechsler, W. Häberle, R. Widmer, H. Rothuizen, P. Vettiger, and J. Thaysen, "Planar Micromagnetic *x/y/z* Scanner with Five Degrees of Freedom", in *Magnetic Materials, Processes, and Devices: Applications to Storage and Micomechanical Systems (MEMS)*, L. Romankiw, S. Krongelb, and C. H. Ahn, Eds., Vol. 98-20, The Electrochemical Society, Pennington, NJ, 1999, pp. 423-433.
[6] H. Rothuizen, U. Drechsler, G. Genolet, W. Häberle, M. Lutwyche, R. Stutz, R. Widmer, P. Vettiger, "Fabrication of a Micromachined Magnetic X/Y/Z Scanner for Parallel Scanning Probe Applications", Microelectronic Eng. 53, 509-512 (2000).
[7] J.-J. Choi, H. Park, K. Y. Kim, J U Jeon, "Electromagnetic Micro x-y Stage for Probe-Based Data Storage", J. Semiconductor Technol. Sci. 1, 84 (2001).
[8] H. Lorenz, M. Despont, N. Fahrni, J. Brugger, P. Vettiger, and P. Renaud, "High Aspect Ratio, Ultrathick, Negative Tone near UV Photoresist and its Applications for MEMS", Sensors and Actuators A 64, 33-39 (1998).
[9] Sylgard 184 silicon elastomer, Dow Corning, Midland, MI.
[10] C. Q. Davis, D. Freeman, "Using a Light Microscope to Measure Motions with Nanometer accuracy", Opt. Eng. 37(4), 1299-1304 (1998). The equipment used is a Networked Probe Station from Umech Technologies.